Pharmaceutical Research, Vol. 26, No. 9, September 2009 (© 2009)
DOI: 10.1007/s11095-009-9921-3

Research Paper

Powder Dissolution Method for Estimating Rotating Disk Intrinsic Dissolution Rates of Low Solubility Drugs

Konstantin Tsinman,[1] Alex Avdeef,[1,2] Oksana Tsinman,[1] and Dmytro Voloboy[1]

Received February 3, 2009; accepted May 29, 2009; published online June 19, 2009

Purpose. The objective was to investigate the applicability and limitations of a novel approach for measuring intrinsic dissolution rates (IDR) of very small quantities of compounds introduced as powders to buffered solutions and comparing these results to disk IDR obtained using the traditional Wood's apparatus.
Methods. The powder dissolution profiles of 13 model drugs were determined at 37°C in USP buffers at pH 1.2, 4.5, and 6.8, stirred at 100 RPM. As little as 0.06 mg of drug were added to 1 mL buffer media. Drug concentration was measured by an *in situ* fiber optic UV method. The results were converted to rotating disk IDR values by a novel mathematical procedure.
Results. The comparison of the powder-based IDR values to those obtained by traditional Wood's apparatus indicated $r^2=0.97$ (n=26).
Conclusion. The results demonstrate that using potentially 10,000-fold less drug material does not sacrifice the quality of the measurement, and lends support to an earlier study that the disk IDR measurement may possibly serve as a surrogate for the BCS solubility classification.

KEY WORDS: Biopharmaceutics classification system; Low solubility; Powder IDR; Rotating disk intrinsic dissolution rate; Wood's apparatus.

INTRODUCTION

Dissolution, solubility, permeability, and pH are core components of the Biopharmaceutics Classification System (BCS), a regulatory guideline (1) applied to solid-dosage oral drug products in aqueous media in order to predict their *in vivo* intestinal absorption performance (2). In the four-class BCS scheme, a drug is considered to be "low" in solubility when its highest dose does not completely dissolve in 250 mL of aqueous media over the pH range 1.0 to 7.5. Such a drug belongs to Class 2 or 4, depending on the value of its permeability (1-3). Recently, it has been tentatively suggested that a drug with a disk intrinsic dissolution rate (IDR) below 100 μg min^{-1} cm^{-2} could be assigned as low soluble in the BCS scheme (4).

For "practically insoluble" drugs, dissolution and dose are critical factors for predicting the rate and extent of absorption for oral dose products (5). During development, investigative IDR studies can be carried out with the traditional Wood's apparatus (4-8), consisting of rotating disks of compacted powder (~500 mg) of the active pharmaceutical ingredient (API) immersed in dissolution test media. Traditional six-vessel US Pharmacopeia (9) (USP) - specified dissolution baths are commonly used, accommodating thermostated (37°C) media (900 mL) in each vessel. Disk IDR values are defined as (4,10) $IDR=DR_{disk}^{max}/A_{disk}$, where A_{disk} is the exposed area (~0.5 cm^2) of the API-containing disk, and DR_{disk}^{max} is the maximum dissolution rate. The feasibility of using IDR measurements (based on traditional USP-type equipment) to determine BCS solubility class membership was investigated by Yu *et al.* (4) using 15 model drugs (6 with low, 9 with high solubility).

However, at the earliest stages of drug development, there is often a shortage of the candidate material to do the dissolution testing using traditional USP-type apparatus. Thus, API-sparing methods are critical to early adoption of dissolution testing (11-13). Additionally, these methods need to be media-sparing as well, especially when simulated intestinal fluid or human intestinal fluid is used.

A miniaturized version of the rotating disk IDR apparatus, using 10 mL volumes and 0.07 cm^2 exposed-area disks with 100-fold reduced quantity of API (compared to traditional methods), has been recently described (11). The miniaturized-apparatus disk IDR values were compared to those determined by traditional equipment (taken from several studies) yielding a correlation coefficient $r^2=0.99$ (n=31) (11). The API concentrations in the miniaturized apparatus were monitored in real time by an *in situ* dip-probe fiber optic UV method (11-14).

Given the promising results from the miniaturized apparatus (11), it was of interest to explore whether the use of powder samples could further reduce the API quantity needed for the testing. Powder IDR values are not commonly

Part 5 in the API-Sparing Dissolution Method series from *p*ION. Avdeef and Tsinman[11] is part 4 in the series.

[1] pION INC, 5 Constitution Way, Woburn, Massachusetts 01801, USA.
[2] To whom correspondence should be addressed. (e-mail: aavdeef@pion-inc.com)

reported; such values generally depend on particle size and are thought to require complicated computational methods to account for the diminishing surface area of dissolving particles, especially those with non-isometric shapes (15-18).

The present study addresses the possibility that the results of qualified powder dissolution measurement can be transformed into USP-type rotating disk IDR values without prior knowledge of the powder-specific surface area or shape or particle size distribution. Thirteen compounds were studied with the novel powder-based method, using as little as 0.06 mg API in 1 mL of pH 1.2, 4.5, and 6.8 buffer media. A biexponential dissolution equation was used to analyze powder dissolution curves.

The objective of the study was to demonstrate that, when applied to low soluble compounds (i.e., IDR $\leq$ 100 μg min^{-1} cm^{-2}), the powder dissolution method can derive IDR values of comparable accuracy as those obtained by traditional Wood's apparatus, but much more quickly and with potentially up to 10,000-fold less API in comparison to the weights suggested by Yu *et al.* (4) for traditional disk IDR apparatus.

MATERIALS AND METHODS

Drugs and Chemicals

Carbamazepine, dipyridamole, furosemide, glibenclamide, griseofulvin, haloperidol, hydrochlorothiazide, indomethacin, ketoprofen, 2-naphthoic acid, naproxen, phenazopyridine hydrochloride, and piroxicam were purchased from Sigma-Aldrich (St. Louis, MO, USA). Standard buffers at pH 1.2 (85 mM HCl, 50 mM KCl), 4.5 (28 mM acetic acid, 22 mM sodium acetate, NaOH), and 6.8 (50 mM KH_2PO_4, NaOH) were made according to the USP Vol. 32 procedures (9).

Miniaturized Pellet Compression System

The Mini-IDR compression system (Heath Scientific, UK) was used to make miniaturized pellets (11). As little as 5 mg of the API powder is loaded into the cylindrical hole of a passivated stainless steel die and compressed (1 min at 120 bar) to a uniform, flat surface with an exposed area of 0.07 cm^2. The die can accommodate larger amounts of API, if needed. Once compressed, the sample die is inserted into a Teflon cylindrical rotating disk carrier containing an embedded magnetic stir bar at its base. The design of the die avoids complications due to edge effects (19) in the original Wood's design (6). The stirrer-die assembly is placed in a 25 mL flat-bottomed glass vial ready for dissolution analysis.

Miniaturized Bath and *In Situ* Fiber Optic Dip-Probe UV Detection

The μDISS Profiler*PLUS* instrument (*p*ION) used in the powder and miniaturized-disk dissolution measurements employs up to eight internal photodiode array (PDA) spectrophotometers, each with its own dedicated fiber optic dip probe, center-positioned in either 4 mL or 25 mL vials seated in a thermostated metal block. The larger vials contain 10 mL of media, with sample pellets fixed in rotating mini-die carriers; the smaller vials are used for powder samples suspended in 1 mL of media stirred by rotating magnetic disks. Stirring speed was set at 100 ± 2 RPM and the temperature was set at 37 ± 0.5 C. Spectral scans (200 – 720 nm) of all eight channels takes less than half a second. The PDA baseline noise is ±0.0002 absorbance units. Concentrations were determined by considering area-under-the-curve (AUC) in second derivative spectra, evaluated over a range of wavelengths. Interference due to background turbidity in powder measurements is minimized by this spectral method (11-14).

THEORETICAL METHODS

The mechanistic modeling of powder dissolution covers a vast literature (20). The treatments are most often framed in terms of the Noyes-Whitney (10) or the Nernst-Brünner (21, 22) equation. The earliest and the simplest of such models was introduced by Hixson and Crowley in 1931, (23) and it is often termed the "cube root law." Many improvements to the model were introduced since then (24-28).

According to the thin film theory (21,22), there is a stagnant layer of solvent adhering to the surface of a solid compound immersed in an aqueous medium. The thickness of this aqueous boundary layer (ABL) is denoted as h. The concentration of the compound at the solid-liquid interface is equal to the solubility, S, of the compound. The diffusional transport of the dissolving compound across the ABL is the rate limiting process in dissolution, according to the classical theory. The compound concentration across the ABL decreases from S at the solid surface to C in the bulk solution.

Curve Fitting Concentration-Time Profiles of Dissolving Powder using a Biexponential Equation

In this study, powder dissolution data were curve-fitted with a biexponential equation, as suggested by the Tinke *et al.* (27) study:

$$C_{tot}(t) = C_0^{\infty} \cdot \left[1 - e^{-k_0 \cdot (t - t_{LAG})}\right] + C_1^{\infty} \cdot \left[1 - e^{-k_1 \cdot (t - t_{LAG})}\right] \quad (1)$$

It is assumed that a saturated solution is present in the time interval of analysis (dose number>1). The derivative of Eq. (1) with respect to time, evaluated at $t=t_{LAG}$ (start of dissolution), is set equal to the limiting slope in the Nernst-Brünner equation:

$$\frac{dC_{tot}(t_{LAG})}{dt} = k_o C_0^{\infty} + k_1 C_1^{\infty} = \frac{A_{app}}{V} \cdot \frac{D}{h_{app}} \cdot S \quad (2)$$

from which the ratio of the apparent total surface area, A_{app}, and the apparent thickness of the ABL, h_{app}, at the start of dissolution process is defined as

$$\left(\frac{A_{app}}{h_{app}}\right) = \frac{V}{DS} \cdot \left(k_0 C_0^{\infty} + k_1 C_1^{\infty}\right) \quad (3)$$

In the above expressions, $C_{tot}(t)$ is the total concentration (μg mL^{-1}) of the dissolved drug as a function of time, t (min). Rigorously, the k_0 and k_1 (min^{-1}) terms are expected to be

time dependent, but for the purpose of the treatment here, they are assumed to be constants. This is a helpful assumption when the "dose number" (2) in the dissolution experiment is sufficiently greater than one (so that a saturated solution forms at t=∞). D($cm^2 min^{-1}$) is the diffusivity of the drug in the medium, V (cm^3) is the volume of the medium, and S (μg mL^{-1}) is the solubility of the drug. C_0^∞ and C_1^∞ are concentrations at t = ∞ of the dissolved particles originating from each of the two parts in Eq. (1). When the dose number >1, $S=C_0^\infty+C_1^\infty$. In Eq. (1), t_{LAG} is a small "lag" time due to experimental timing delays, wettability delays, etc. Nonlinear weighted regression analysis in the μDISS Profiler*PLUS* software was used to determine the five constants associated with Eq. (1): C_o^∞, k_0, C_1^∞, k_1, and t_{LAG}.

Using Powder Dissolution Data to Approximate the Rotating Disk Intrinsic Dissolution Rate (IDR)

As noted in the Introduction, investigative dissolution studies are often carried out with rotating disks of the API immersed in dissolution media, using traditional Wood's apparatus. It's an appealing approach: the disk surface area, A_{disk}, is easy to measure, and remains practically constant during dissolution, and hydrodynamics of such a system are well defined (29). In contrast, traditional analysis of powder dissolution data involves more complicated steps (15-28). However, it is the API-sparing nature of powder dissolution that makes its potential use to estimate IDR very attractive, notwithstanding the complications.

When comparing stirred-powder to rotating-disk dissolution, *for the same surface area and stirring speed,* the dissolution rates are generally higher for powders consisting of small particles (<100 μm) than for rotating disks (substantially so under normal conditions). This is because $h_{app} << h_{disk}$ for very small particles (12,15-18). With rotating disks, the diffusion layer thickness, h_{disk}, is time independent. However, in particle suspensions, h_{app} is expected to be a function of time, since it depends on the size of the particles (less than about 100 μm in size), and thus generally decreases during dissolution (15-18,24,26). In this study, conditions were generally set (dose number >>1) to favor the near constancy of the particle size.

The intrinsic dissolution rate based on the rotating disk thin-film model is normally stated as

$$IDR_{disk} = \frac{DR_{disk}^{\max}}{A_{disk}} = \frac{1}{h_{disk}} \cdot DS \tag{4}$$

The intrinsic dissolution rate based on polydisperse powders may be similarly stated as

$$IDR_{pwd} = \frac{DR_{pwd}^{\max}}{A_{app}} = \frac{1}{h_{app}} \cdot DS \tag{5}$$

Equation 5 may be substituted into Eq. (4) to remove the common DS term, to yield

$$IDR_{pwd} = DR_{disk}^{\max} \cdot \left(\frac{h_{app}}{A_{app}}\right) \cdot \frac{1}{h_{disk}} \tag{6}$$

DR_{pwd}^{max} (μg min^{-1}) is the maximum slope in the powder dissolution curve: $C_{tot}(t)\cdot V$ *vs.* t, evaluated at t= t_{LAG}. The apparent h/A ratio is obtained from Eq. (3). The disk ABL thickness, h_{disk} (cm), in Eq. (6) was estimated from the Levich equation (29),

$$h_{disk} = 4.98\ \eta^{\frac{1}{6}} \cdot D^{\frac{1}{3}} \cdot RPM^{-\frac{1}{2}} \tag{7}$$

where RPM (rev min^{-1}) is the rotation speed, and η is the solvent kinematic viscosity (0.00696 $cm^2 sec^{-1}$ in aqueous solution at 37° C). The diffusivity ($cm^2 sec^{-1}$ units in Eq. 7) was estimated from the molecular weight (MW), according to the empirical formula (37°C) (30): $D=1.339 \cdot 10^{-4.15-0.448 \log MW}$. The latter equation, along with Eqs. (3) and (7), are then rolled into Eq. (6), to produce the following expression to approximate traditional rotating disk IDR, using data obtained from powder measurements (37°C):

$$IDR_{disk}(\mu g\ \min^{-1} cm^{-2}) = 0.0573 \frac{DR_{pwd}^{\max}}{V} \cdot MW^{-0.30} \cdot \sqrt{RPM} \cdot \left(\frac{C_0^\infty + C_1^\infty}{k_o C_0^\infty + k_1 C_1^\infty}\right) \tag{8}$$

RESULTS AND DISCUSSION

Analysis of Powder Dissolution Data using the Biexponential Equation

Table I lists the diffusivities and the h_{disk} values of the compounds. Table II summarizes the results of the biexponential equation (Eq. 1) analysis of the powder dissolution data. With the exception of ketoprofen, all compounds in the study were added with a dose number>1, so that at the end of the dissolution period, some solid remained in the media (cf., %D in Table II). In the case of ketoprofen (dose number slightly below one), only the data in the early portion of the dissolution curve (containing excess solid) were subjected to the regression analysis, using a single-exponential (three-parameter) form of Eq. (1).

Powder Dissolution Profiles

Fig. 1 shows the powder dissolution curves for the several of the compounds analyzed in the study. Up to six replicate dissolution experiments (cf., Table II) were performed for each compound. The averaged concentrations, along with the standard deviations (SD) at each time point, are displayed in Fig. 1. The solid curves in each frame of the figure represent fitting of the dissolution data to Eq. (1). Table II lists the refined parameters resulting from the analysis. Table II lists the IDR and the solubility values calculated from the biexponential equation parameters, as described in the Theoretical Methods section. The disk IDR values determined here spanned nearly 3 orders of magnitude (0.14 to 97 μg $min^{-1} cm^{-2}$).

Dissolution profiles for dipyridamole (Fig. 1b) and piroxicam (Fig. 1f) may indicate a polymorph transformation taking place during dissolution. Jinno *et al.* (8) had characterized the effect in the case of piroxicam as that of anhydrous form conversion to the less-soluble monohydrate. The dissolution curve pattern reported by these investigators was

Table I. Properties

COMPOUND	MW	D (cm^2/s)[a]	h_{disk} (μm)[b]
carbamazepine	236.27	8.2E-06	44
dipyridamole	504.64	5.8E-06	39
furosemide	330.75	7.0E-06	42
glibenclamide	494.00	5.9E-06	39
griseofulvin	352.77	6.8E-06	41
haloperidol	375.86	6.6E-06	41
hydrochlorothiazide	297.70	7.4E-06	42
indomethacin	357.79	6.8E-06	41
ketoprofen	254.28	7.9E-06	43
2-naphthoic acid	172.20	9.4E-06	46
naproxen	230.26	8.3E-06	44
phenazopyridine	213.24	8.6E-06	44
piroxicam	331.35	7.0E-06	42

[a] Diffusivity coefficients (37°C, aqueous), calculated according empirical formula (see text)
[b] Thickness of the disk aqueous boundary layer calculated by the Levich Eq.(7) (100 RPM, 37°C, η=0.00696 $cm^2\ sec^{-1}$)

also observed here (Fig. 1f). Since the traditional rotating disk IDR values for piroxicam were based on the kinetics of the anhydrous form (8), the analysis here focused on the dissolution data in the interval up to 40 min. We are not aware of traditional rotating disk IDR values having been published for dipyridamole. Consequently, the miniaturized rotating disk IDR method was used to collect data for dipyridamole, which was then compared with the powder dissolution data. A complicated powder dissolution curve (open circles in Fig. 1b) was observed when a large excess of dipyridamole (0.99 mg per mL) was used, resembling that of piroxicam (Fig. 1f). This may be due to the transformation of the anhydrous form of dipyridamole (S≈8.7 μg mL^{-1}) to a lower-solubility hydrate form (S=5.3 μg mL^{-1}). When the experiment was repeated with a smaller excess of dipyridamole (0.06 mg powder per mL), there appeared to be no indication of the higher-solubility polymorph. The decreased total surface area in the repeated experiment led to a slower rate of dissolution of the anhydrous form. Apparently, as soon as dipyridamole was released from the solid, it converted to the putative hydrate form, perhaps coating the surface in the process. The rate limiting kinetics would then have been due to that of the lower-solubility form of the drug. The miniaturized disk IDR (Table III) results only indicated the lower solubility form. Additional tests are needed to confirm the hydrate formation hypothesis.

Column 6 in Table II lists the (A_{app}/h_{app}) ratios divided by the weight of powder used. It can be seen that they spread almost two orders of magnitude from 108 cm mg^{-1} for 2-

Table II. Biexponential model refinement results[a]

COMPOUND	wt/vol (mg/mL)	%D	C_0^∞ (μg/mL)	C_1^∞ (μg/mL)	$(A/h)_{app}/W_o$ (cm/mg)	GOF	No. Curves
carbamazepine(recryst.), pH1.2,4.5,6.8	0.72	28	125 ± 17	79 ± 15	1856 ± 309	0.5	6
dipyridamole, pH4.5	0.68	26	157 ± 1	19 ± 1	2651 ± 120	0.3	2
dipyridamole, pH6.8	0.065	8	4.4 ± 0.2	0.87 ± 0.57	2471 ± 118	0.3	3
furosemide, pH4.5	0.82	18	128 ± 5	23 ± 4	3562 ± 137	0.3	3
glibenclamide, pH6.5	0.11	2	2.0 ± 0.2	0.26 ± 0.22	395 ± 56	0.8	2
griseofulvin,pH1.2,4.5,6.8	0.11	23	23 ± 1	2.4	6852 ± 370	0.2	4
haloperidol, pH6.8	0.22	19	27 ± 1	15 ± 1	1316 ± 88	0.3	6
hydrochlorothiazide, pH1.2,4.5,6.8	0.98	93	713 ± 26	202 ± 25	559 ± 62	0.4	6
indomethacin, pH4.5	0.13	6	7.1± 0.1	1.3± 0.1	1186± 85	0.5	5
ketoprofen, pH1.2	0.25	100	255± 2	0.0	1148 ±82	0.6	1
ketoprofen, pH4.5	0.53	100	529± 5	0.0	1441± 90	5.6	1
2-naphthoic acid, pH 4.5	1.26	16	192± 1	10.8 ± 0.1	108± 36	0.1	6
naproxen, pH 1.2	0.087	54	41 ±5	6.2± 5.0	2222± 333	1.9	1
naproxen, pH 4.5	0.21	74	140± 1	13± 1	2805± 122	1.1	1
phenazopyridine.HCl,pH 1.2	0.36	89	316± 2	0.0	1120± 80	0.5	6
phenazopyridine.HCl,pH4.5	1.31	14	153± 2	24	9149± 851	0.3	2
phenazopyridine.HCl, pH6.8	0.61	9	8.3± 0.8	47± 1	4265± 294	0.1	6
piroxicam, pH 4.5	0.43	7	7.2± 1.9	23± 2	563± 63	0.1	4

[a] Fit of Eq. (1) to powder dissolution curves. Percentage of the drug dissolved is %D. GOF = goodness-of-fit. No. Curves = number of replicate dissolution curves. Weighting scheme based on standard deviations at each point from averaging multiple dissolution curves; unit weights used for ketoprofen and naproxen. Parameters without standard deviations were treated as fixed (unrefined) contributions. Average t_{LAG}=0.18±0.35 min

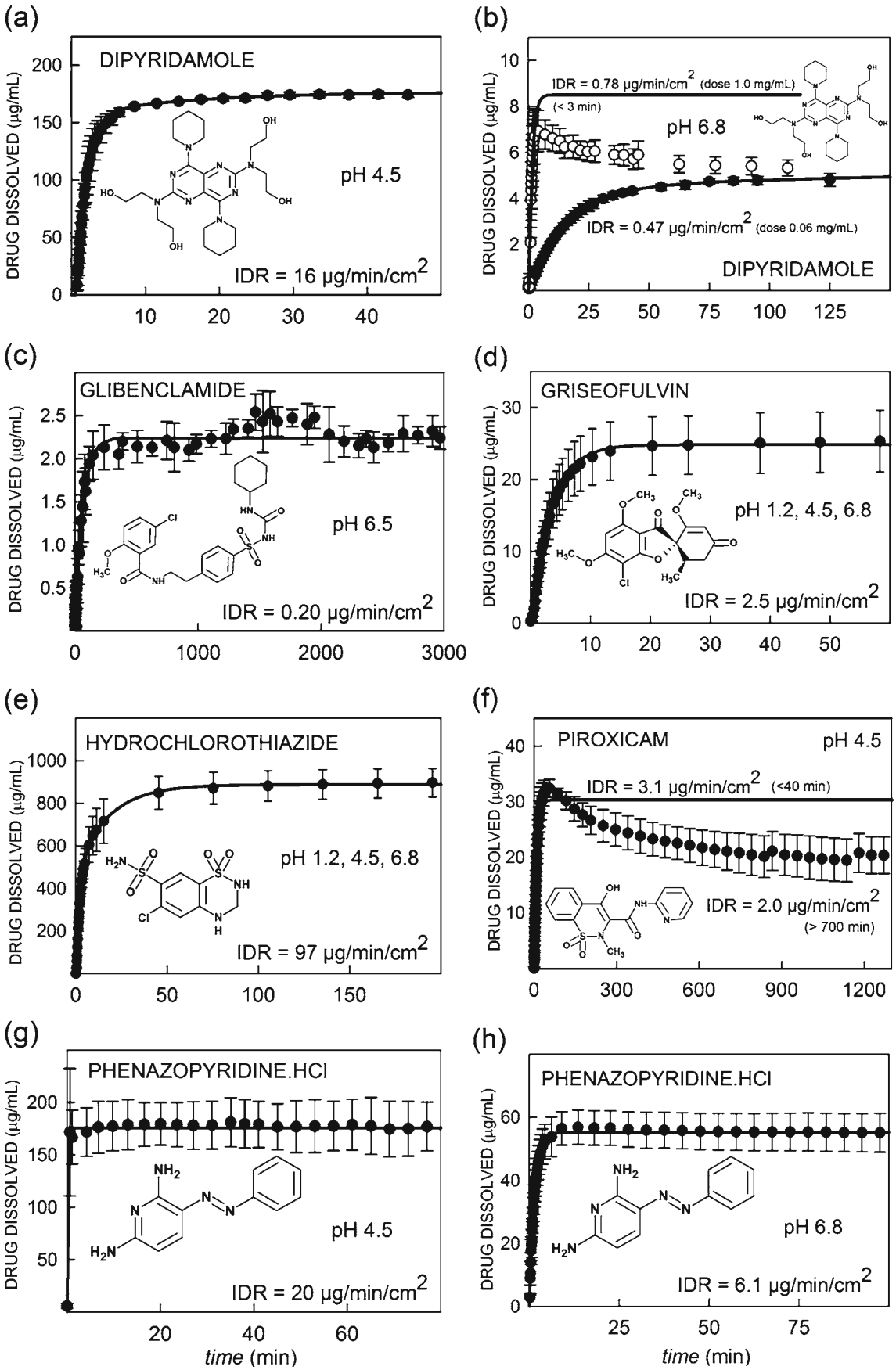

Fig. 1. Powder dissolution profiles at 37°C, 100 RPM stirring. The solid lines are best-fit curves, based on the biexponential expression, Eq. (1). The IDR values listed in the figure were determined with powder data, using Eq. (8).

Table III. Comparison of IDR values (37°C, 100 RPM)

COMPOUND	pH	S[a] (μg mL^{-1})	IDR based on powder data[b] (μg min^{-1} cm^{-2})	*disk* IDR miniaturized[c] (μg min^{-1} cm^{-2})	*disk* IDR traditional[d] (μg min^{-1} cm^{-2})
carbamazepine (recryst.)	1.2, 4.5, 6.8	205± 23	23± 3	21[e]	26[g]
dipyridamole	4.5	177± 1	16± 1	13± 1[f]	
	6.8	5.3± 0.6	0.47± 0.05	0.41± 0.02[f]	
furosemide	4.5	151± 7	15±1	20[e]	18[g]
glibenclamide	6.5	2.3± 0.3	0.20± 0.03	0.14 ± 0.01[f]	
griseofulvin	1.2, 4.5, 6.8	25± 1	2.5± 0.1	1.9[e]	2.2[g]
haloperidol	6.8	41± 1	4.0± 0.1	2.6±0.1[f]	
hydrochlorothiazide	1.2, 4.5, 6.8	915± 36	97± 4	97[e]	119[g]
indomethacin	4.5	8.4± 0.2	0.83± 0.02	0.95± 0.02[f]	
ketoprofen	1.2	255± 2	29± 1		16[g]
	4.5	529± 5	60± 2	63[e]	62[g]
2-naphthoic acid	4.5	203± 1	25± 1	24± 1[f]	
naproxen	1.2	47± 7	5.3± 0.8		3.5[g]
	4.5	153± 1	17± 1	13[e]	12[g]
phenazopyridine.HCl	1.2	316± 2	35± 1	42± 4[f]	59[h]
	4.5	178± 2	20± 1		15[h]
	6.8	55± 1	6.1± 0.1		3.5[h]
piroxicam (anhydrous)	4.5	30± 2	3.1± 0.2	4.1[e]	4.3[g]

[a] Solubility determined from the powder dissolution data (= $C_0^{\infty} + C_1\infty$)
[b] Intrinsic dissolution rate (IDR) determined from powder data, using Eq. (8)
[c] IDR determined from miniaturized rotating disk apparatus, following the method described in ref. (11)
[d] IDR determined by traditional Wood's apparatus, with protocols defined in the USP
[e] Ref. (11)
[f] This work
[g] Ref. (4)
[h] Ref. (7); literature data at 200 RPM—IDR corrected to 100 RPM (dividing by √2)

naphthoic acid to 9149 cm mg^{-1} for phenazopyridine.HCl at pH 4.5. This parameter plays an important role in determining the dissolution rate of powder and it could be reasonable to assume that the larger this parameter is, the smaller the particles that are introduced into the dissolution medium.

Miniaturized Disk IDR Data

For those compounds without reported traditional IDR values, new rotating disk measurements were performed in this study, using the miniaturized method (11). The results are summarized in Table III.

Correlation of Powder-Derived IDR Data to that Reported in the Literature Based on Traditional Disk IDR Method

Table III lists the literature IDR values based on traditional and miniaturized Wood's apparatus, as well as the IDR values estimated by the powder method, according to Eq. (8). Fig. 2 is the resultant correlation log-log plot, based on the values in Table III. A very high correlation was achieved in the study, with r^2=0.97 (n=26). It is important to note that this correlation did not include any prior knowledge of the specific surface area and did not involve any assumptions about the shape or distribution of the particles when powder dissolution curves were evaluated using Eq. (8). The analysis assumed that k_0 and k_1 in Eq. (1) remained practically constant during the powder dissolution. This appears to be a reasonable assumption for the low solubility compounds (S<1 mg mL^{-1}) under dose number>1 experimental conditions.

Equilibration Time: Powder *vs.* Miniaturized Rotating Disk Dissolution

Besides being API-sparing in nature, powder dissolution also is appreciably time-sparing, in comparison to traditional

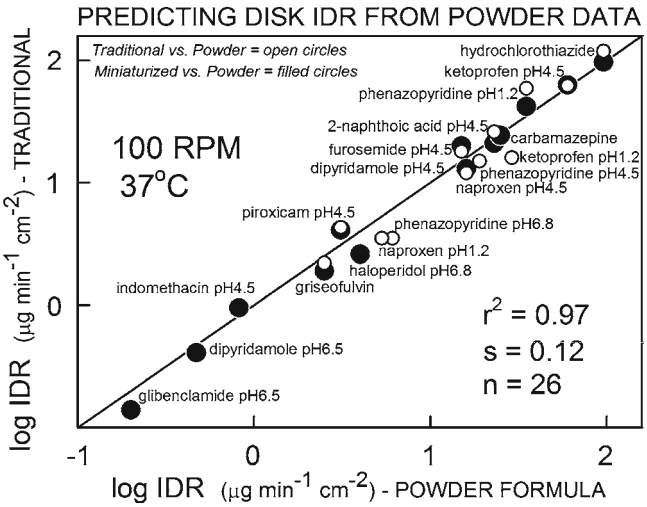

Fig. 2. Log-log correlation diagram, comparing published disk IDR values determined by traditional and miniaturized rotating disk apparatus *vs.* values determined in this study, using powder data.

rotating disk IDR methods. The half-saturation times, $t_{1/2}$, can be obtained by setting C(t)/S to 0.5 in Eq. (1), and solving for the half-time. For example, in the griseofulvin miniaturized rotating disk dissolution, it takes over 10 h to reach the half-saturation point; for powder dissolution, $t_{1/2}$ is reached in about 2 min. With the compounds studied, the powders released the drug from 15 (ketoprofen pH 4.5) to 600 (carbamazepine) times faster than the miniaturized rotating disks. Most of the powders dissolved about 100 times faster than the corresponding disks (data not shown).

Fig. 3 shows the miniaturized rotating disk dissolution profile of phenazopyridine hydrochloride at pH 1.2, taken over 7 days. The inset curve represents powder dissolution, taken over 35 min. The disadvantage of long exposures in miniaturized rotating disk experiments is that the compound may decompose. Comparisons of the sample phenazopyridine spectra to those taken during the standard calibration procedure indicated that there was some decomposition evident after about 40 h of dissolution. The analysis reported here was based only on the rotating disk data in the first 40 h of dissolution.

The Reliability of Solubility Determination in the Powder Method

Since we restricted the powder-based IDR method to dose numbers>1, normally, a saturated solution is present at the end of dissolution, as the process is poised at equilibrium. At that time, the concentration of the API is thus equal to its solubility (at the pH in the saturated solution, *which may be different from the starting pH of the medium,* as discussed elsewhere (11)). The *in situ* fiber optic UV method determines the concentration of the API at all times, and thus the concentration at the end of the dissolution interval is equal to the solubility. Only in the case of ketoprofen was the dose number slightly underestimated, and the sample completely dissolved at very long times. It was necessary to restrict the data for analysis to be during the time when excess solid was still present. The solubility of ketoprofen (but not any of the other compounds in the study) was thus *predicted* using Eq. (1). The empirical equation cannot be applied to a perfectly linear concentration-time curve. The more bend there is in the curve, the better is the prediction of solubility. In the case of ketoprofen, there was enough bending in the curve to predict S(pH 1.2)=255 μm/mL and S(pH 4.5)= 529 μg/mL (Table III). From Sheng *et al.* (31) S (pH 4.0)= 280 μg/mL and S(pH 4.6)=490 μg/mL. This is reasonable agreement (the pK_a of ketoprofen is 4.02 (11)), suggesting that even the prediction of solubility is sufficiently reliable under the selected experimental conditions.

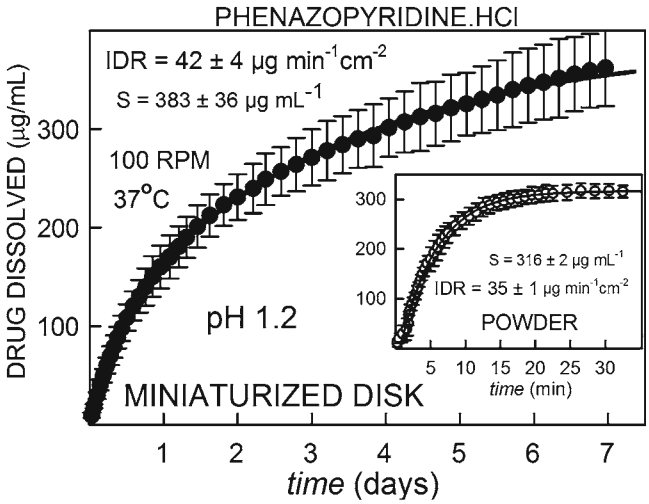

Fig. 3. Comparison of the times required to reach equilibrium for phenazopyridine hydrochloride (pH 1.2, 37°C, 100 RPM) in the miniaturized rotating disk method and the (inset) stirred powder method. The powder dissolved almost 300 times faster than the miniaturized rotating disk.

As the previous paper in the API-sparing series indicated (11), the pH at the surface of dissolving ionizable weak acids/bases can be quite different from that of the bulk medium. For example (11), for atenolol dissolving in the pH 6.8 USP buffer, the pH at the solid-liquid interface is about 9.5. Since the solubility term in the Nernst-Brünner equation refers to the solid-liquid interfacial pH, not bulk-medium pH, it can be misleading to associate the determined solubility—and thus the IDR—to the nominal pH of the buffer. This is a potential problem for highly soluble compounds suspended in media of low buffer capacity, as the previous study indicated. But as suggested then, this problem may be overcome by measuring the pH at the end of dissolution (under dose number>1 conditions). For low soluble compounds, however, the solubility values in Table III do correspond closely to the values expected in the pH of the media, since the amount of compound dissolved is not enough to cause the surface pH to be appreciably different from the bulk medium pH.

Although the powder-based IDR method described here is most accurate for classifying low solubility compounds, it can still be used for solubility designation, since the method is accurate enough to predict the location of the low-high boundary.

CONCLUSION

Our objective was to determine how well the powder dissolution approximation of IDR correlates to high-quality rotating disk IDR data based on the traditional (4, 8) and miniaturized (11) Wood's apparatus. Our study suggests that the objective was met with the compounds studied. *No prior knowledge of the powder-specific surface area or particle shape or size distribution was required.* Powder dissolution experiments did not require sink conditions to be maintained as the entire dissolution curve was used in deriving disk IDR values. By demonstrating that the quantity of API used in traditional rotating disk apparatus could be reduced by potentially 10,000-fold without sacrificing the quality of the measurement, we are confident that the opportunity to consider investigative dissolution studies earlier in drug development is possible in projects where only a few mg of API may be available for evaluation.

ACKNOWLEDGMENT

We thank Christel Bergström and Per Artursson of Uppsala University and Per Nielsen of *p*ION for helpful

discussions and suggestions regarding the API-sparing dissolution methodology.

REFERENCES

1. Guidance for Industry. Waiver of *In Vivo* Bioavailability and Bioequivalence Studies for Immediate Release Solid Oral Dosage Forms Based on a Biopharmaceutics Classification System. Washington, D.C., USA: FDA; 2000.
2. Amidon GL, Lennernäs H, Shah VP, Crison JR. A theoretical basis for a biopharmaceutic drug classification: the correlation of *in vitro* drug product dissolution and *in vivo* bioavailability. Pharm Res. 1995;12:413–420.
3. Kostewicz ES, Wunderlich M, Brauns U, Becker R, Bock T, Dressman JB. Predicting the precipitation of poorly soluble weak bases upon entry in the small intestine. J Pharm Pharmacol. 2004;56:43–51.
4. Yu LX, Carlin AS, Amidon GL, Hussain AS. Feasibility studies of utilizing disk intrinsic dissolution rate to classify drugs. Int J Pharm. 2004;270:221–227.
5. Dressman JB, Amidon GL, Reppas C, Shah VP. Dissolution testing as a prognostic tool for oral drug absorption: immediate release dosage forms. Pharm Res. 1998;15:11–22.
6. Wood JH, Syarto JE, Letterman H. Improved holder for disk intrinsic dissolution rate studies. J Pharm Sci. 1965;54:1068.
7. Serajuddin ATM, Jarowski CI. Effect of diffusion layer pH and solubility on the dissolution rate of pharmaceutical bases and their hydrochloride salts I: phenazopyridine. J Pharm Sci. 1985;74:142–147.
8. Jinno J, Oh D-M, Crison JR, Amidon GL. Dissolution of ionizable water-insoluble drugs: the combined effect of pH and surfactant *J*. Pharm Sci. 2000;89:268–274.
9. The United States Pharmacopeia (USP 32). United States Pharmacopeial Convention, Inc., Rockville, MD, 2009.
10. Noyes AS, Whitney WR. The rate of solution of solid substances in their own solutions. J Amer Chem Soc. 1897;19:930–934.
11. Avdeef A, Tsinman O. Miniaturized rotating disk intrinsic dissolution rate measurement: effects of buffer capacity in comparisons to traditional Wood's apparatus. Pharm. Res. 2008;25:2613–2627.
12. Avdeef A, Tsinman K, Tsinman O, Sun N, Voloboy D. Miniaturization of Powder Dissolution Measurement and Estimation of Particle Size. *Chem. Biodiv.* **2009**. *In press*.
13. Avdeef A. Solubility of sparingly-soluble drugs. Dressman J, Reppas C. (Eds., special issue: The Importance of Drug Solubility). *Adv. Drug Deliv. Rev.* **2007**, *59*, 568–590.
14. Bijlani V, Yuonaye D, Katpally S, Chukwumezie BN, Adeyeye MC. Monitoring ibuprofen release from multiparticulates: *in situ* fiber-optic technique *versus* the HPLC method. *AAPS Pharm. Sci.Tech.* **2007**, *8*, Article 52 (http://www.aapspharmscitech.org).
15. Pedersen PV, Brown KF. Theoretical isotropic dissolution of nonspherical particles. J Pharm Sci. 1976;85:1437–1442.
16. Carstensen JT, *Advanced Pharmaceutical Solids*. Marcel Dekker, New York, 2001, pp. 51–88, 191–208.
17. Mosharraf M, Nyström C. The effect of particle size and shape on the surface specific dissolution rate of micronized practically insoluble drugs. Int J Pharm. 1995;122:35–47.
18. Galli C. Experimental determination of the diffusion boundary layer with micron and submicron particles. Int J Pharm. 2006;313:114–122.
19. Jashnani RN, Byron PR, Dalby RN. Validation of an improved Wood's rotating disk dissolution apparatus. J. Pharm. Sci. 1993;82:670–671.
20. Dokoumetzidis A, Macheras P. A century of dissolution research: from Noyes and Whitney to the Biopharmaceutics Classification System. Int J Pharm. 2006;321:1–11.
21. Nernst W. Theorie der reaktionsgeschwindigkeit in heterogenen systemen. Z Phys Chem. 1904;47:52–55.
22. Brünner E. Reaktionsgeschwindigkeit in heterogenen systemen. Z Phys Chem. 1904;47:56–102.
23. Hixson A, Crowell J. Dependence of reaction velocity upon surface and agitation. I. Theoretical considerations. Ind Eng Chem. 1931;23:923–931.
24. Higuchi WI, Hiestand EN. Dissoluiton rates of finely divided powders I. Effect of particle sizes in a diffusion process. J Pharm Sci. 1963;52:67–71.
25. Pedersen PV, Brown KF. General class of multiparticulate dissolution models. J Pharm Sci. 1975;64:1435–1438.
26. Lu AT, Frisella ME, Johnson KC. Dissolution modelling: factors affecting the dissolution rates of polydisperse powders. Pharm Res. 1993;10:1308–1314.
27. Tinke AP, Vanhoutte K, De Maesschalck R, Verheyen S, De Winter H. A new approach in the prediction of the dissolution behaviour of suspended particles by means of the particle size distribution. J Pharm Biomed Anal. 2005;39:900–907.
28. Okazaki A, Mano T, Sugano K. The theoretical model of polydisperse drug particles in biorelevant media. J Pharm Sci. 2008;97:1843–1852.
29. Levich VG. Physiochemical Hydrodynamics. Englewood Cliffs, N. J: Prentice-Hall; 1962. p. 39–72.
30. Avdeef A, Absorption and Drug Development. Wiley-Interscience. NJ: Hoboken; 2003.
31. Sheng JJ, Kasim NA, Chandrasekharan R, Amidon GL. Solubilization and dissolution of insoluble weak acid, ketoprofen: effect of pH combined with surfactant. Eur J Pharm Sci. 2006;29:306–314.